

Article

Management of Dredging Activities in a Highly Vulnerable Site: Simulation Modelling and Monitoring Activity

Diana De Padova *, Mouldi Ben Meftah , Francesca De Serio  and Michele Mossa 

Department of Civil, Environmental, Land, Building Engineering and Chemistry (DICATECh), Polytechnic University of Bari (Italy), via Orabona 4, 70125 Bari, Italy; mouldi.benmeftah@poliba.it (M.B.M.); francesca.deserio@poliba.it (F.D.S.); michele.mossa@poliba.it (M.M.)

* Correspondence: diana.depadova@poliba.it

Received: 27 October 2020; Accepted: 8 December 2020; Published: 13 December 2020



Abstract: Unfortunately, more and more contaminants, such as heavy metals and other organic micro-pollutants, degrade the good ecological status of marine systems. The removal of contaminated sediments from harbours through dredging activities may cause harmful changes in the environment. This present work shows how monitoring the activity and validated numerical models can be of great help to dredging activities that can cause environmental impacts due to the increase of the suspended solid concentration (SSC) and their dispersion and deposition far from the dredging point. This study is applied to a hypothetical dredging project in a very vulnerable coastal site in Southern Italy, the Mar Piccolo Basin. A statistical analysis of the simulated parameter SSC was carried out to numerically estimate its spatial (vertical and horizontal) variability, thereby allowing an evaluation of the potential environmental effects on the coastal area.

Keywords: 3D numerical modelling; field measurements; semi-enclosed basin; sea currents; dredging management; environmental effects

1. Introduction

In the last years, the problem of contaminated marine sediments has become a worldwide environmental issue, because it threatens the marine systems and human health. However, contamination often involves large volumes of sediment but with low contamination levels; in this case, “no action” may be a preferred alternative in cases in which the remedy may be worse than the disease [1].

However, when dredging is a fundamental element of the economic/environmental performance of a basin, it is very important to define an environmental monitor strategy to assess the state of the marine ecosystem in order to avoid any adverse effects to the environment and prepare also the eventual adoption of mitigation measures.

All types of dredging operations create turbidity in the water column, depending on the type of dredges (hydraulic or mechanical), of the sediment bed and hydrodynamic conditions.

The most important environmental problems on marine organisms are reductions in dissolved oxygen and the decrease of sunlight in surface water due to turbidity.

In the last years, increasing attention has been paid to environmental impacts during dredging activities, and therefore, mitigating measures to reduce these effects have been adopted [2].

This has led to the development of new types of ecological dredges in order to reduce suspended sediment and turbidity, especially to remove and to relocate contaminated materials. In particular, special watertight buckets called “environmental” buckets are used to reduce the turbidity of dredging operations in the presence of contaminated sediments [3–6].

As shown by previous studies [7–11], heavily anthropized coastal basins can be a very vulnerable site, thus requiring strict monitoring actions by local authorities and stakeholders. Therefore, the monitoring activity is a useful tool to assess the status of an environment, mostly in sensitive coastal sites characterised by anthropic pressure factors. The synergistic use of numerical models and monitoring activity can facilitate decision-making during an environmental dredging activity [12]. However, all these numerical models need to be calibrated with reliable field data to have consistent and accurate results.

It is important to define quantifiable tolerance limits for the suspended solid concentration (SSC) as supporting environmental studies and the subsequent indirect monitoring and modelling in a management context during a dredging activity. In this paper, we focused our attention on a coastal site considered one of the most polluted marine ecosystems in Europe.

More recent research paid attention to the hydrodynamic, hydrology, geology and topography characterisations of the area in order to estimate the potential environmental impacts induced by dredging activities [13–16].

This paper is organised as follows: firstly, a thorough calibration of a 3D hydrodynamic flow model is performed using a set of measured data; after this, a transport module is coupled to the hydrodynamic model to study the response of the basin to a hypothetical dredging activity.

2. Materials and Methods

2.1. Study Site

The Mar Piccolo of Taranto, located in Southern Italy (Ionian Sea), is a complex marine ecosystem model important in terms of ecological, social and economic activities for the presence also of extensive mussel farms [17] (Figure 1). It is composed of two bays and joined to the external basin named Mar Grande by means of two channels, i.e., the Navigable Channel and the Porta Napoli Channel. The two bays of the Mar Piccolo are considered as two different ecosystems influencing each other, and the Mar Piccolo basin was assimilated into an estuary by many authors [18–20].



Figure 1. Target area.

The area of the Mar Piccolo Basin is roughly 20.72 km² and is characterised by the presence of a large number of submarine springs and of two small rivers, called Galeo into Bay I and Ajedda into Bay II. The maximum depth is about 12 m in Bay I and about 9 m in Bay II.

Mar Piccolo, with typical lagoon features and with a suffering scarce circulation, is extremely vulnerable, and unfortunately, this area is characterised to continue the release and diffusion of contaminants with strong chemical–ecological risks towards the marine ecosystem and

human health [21–26]; therefore, it is important to test potential remediation strategies for contaminated sediments.

The lagoon features of the Mar Piccolo are mainly due to the presence of 34 submarine freshwater springs (locally called “citri”), of which 20 are in the first inlet and 14 in the second inlet.

2.2. Environmental Monitoring Action

Environmental monitoring in the Mar Grande and Mar Piccolo of Taranto includes two fixed stations briefly described below (Figure 2).



Figure 2. Location of the fixed monitoring stations in the target area.

In the Mar Grande Basin (Figure 3), a bottom-mounted acoustic doppler current profile (ADCP); a multidirectional wave array; a weather station and a CTD (measuring water conductivity, water temperature and depth) were installed. In the Navigable Channel, a second bottom-mounted ADCP and a wave array were installed (Figure 2). More details on the stations can be found in De Serio and Mossa [27].



Figure 3. Seamount where the monitoring station in Mar Grande was installed.

Moreover, some field data were collected by using a Nortek AWAC vessel-mounted acoustic doppler current profiler (VM-ADCP) on 26 November 2014 between 9:30 a.m. and 13:00 p.m. (GMT) by the research group of the Department of Civil, Environmental, Land, Building Engineering and Chemistry of the Polytechnic University of Bari (Italy) in the frame of the RITMARE Project. Figure 4 shows the points where the measurements were assessed.

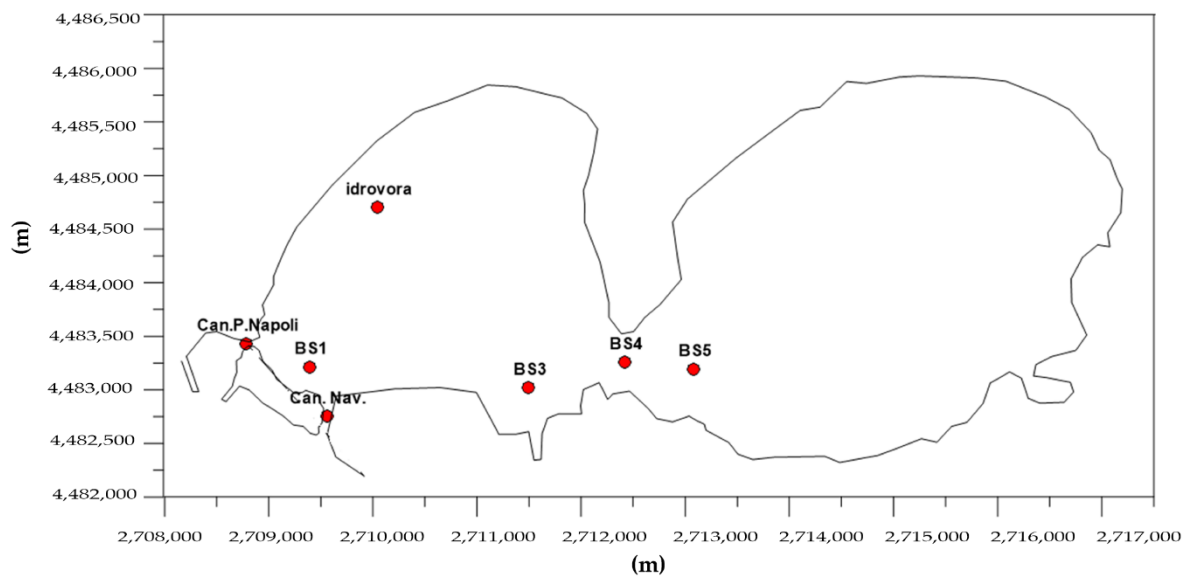


Figure 4. Displacement of the stationing points.

The data recorded during the monitoring survey were used to validate the hydrodynamic model.

3. Numerical Simulation

Hydrodynamic and transport modules are used to evaluate how the sea circulation affects sediment transport for different dredging techniques within the target area. In particular, hydrodynamic (HD) and mud transport module (MT) modules of MIKE 3 FM, produced by the Danish Hydraulic Institute (DHI) [28], were used to model the sea current field and the sediment plume dynamics.

3.1. Modelling of Marine Currents and Calibration

The basic characteristics, numerical formulation and process equations of the model MIKE 3 FM are provided by DHI [29]. A finite mesh of 7235 triangular elements with ten vertical layers was used. The simulation was forced at the sea open boundary by the Temperature and Salinity vertical profiles and the $u - v$ velocity vertical profiles extracted by the Mediterranean Sea physics reanalysis model [29]. The atmospheric data (u and v components of wind (m/s), atmosphere pressure (Pa), total cloud cover (%), solar radiation (J/m^2) and air temperature ($^{\circ}C$)) were extracted by ERA5 developed through the Copernicus Climate Change Service (C3S). The precipitation data (mm/d) was extracted by CPC Merged Analysis of Precipitation (CMAP) [30].

A $k-\epsilon$ formulation for the vertical direction [31] and on the Smagorinsky formulation for the horizontal direction [32] were used.

Figure 5 shows the comparison between the computed motion field (grey vectors) and the measurements (red vectors). For the sake of brevity, only two selected depths are shown, i.e., -4 m and -7 m.

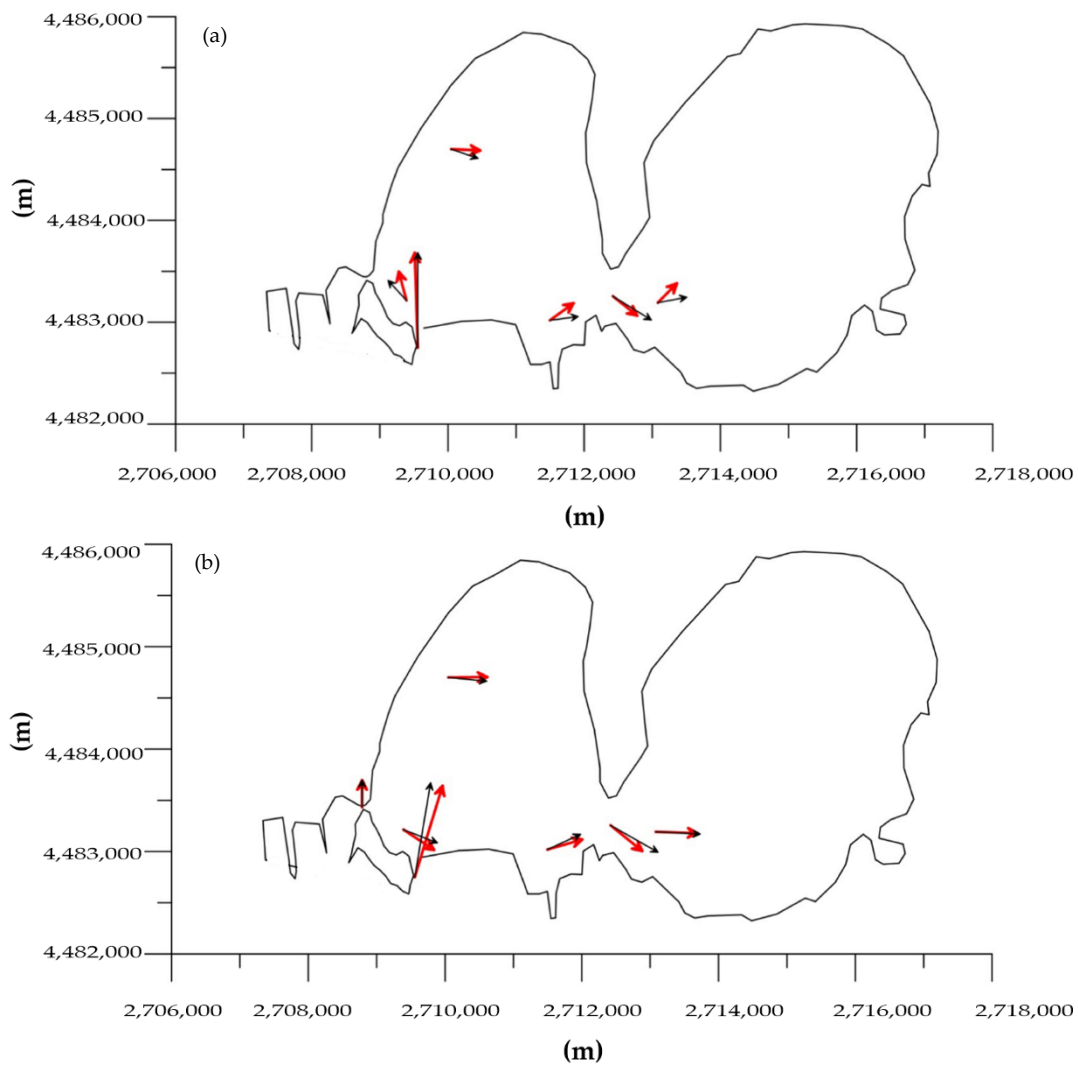


Figure 5. Comparison between the numerical and the measured flow fields on 26 November 2014. Red vectors are the measured velocities, while the black ones are the modelled velocities at (a) $z = -4$ m and (b) $z = -7$ m.

3.2. Mud Transport Modelling

The mud transport module (MT) coupled with the validated hydrodynamic model (HD) were used. It is able to reproduce the SSC spatial and temporal evolution during a hypothetical dredging activity in an area of 50 ha with a bed thickness equal to 50 cm (Figure 6). For more details on this module (MT), the reader can refer to [33,34].

The Mar Piccolo is mainly characterised by silty bottom sediments (particle diameter $d < 0.004$ mm) with medium consolidation; consequently, a critical shear stress $\tau_{ce} = 0.2$ N/m² was derived for these sediments [28]. In the present work, we used a value of the coefficient of erodibility E equal to 1×10^{-4} kg/s/m², following [28].

Therefore, two simulation runs, denoted as T1 and T2, were carried out with the aim of comparing the effects due to a conventional hydraulic dredge and an environmental mechanical dredge.

The dredging activity was modelled over a period of 12 days, starting on 2 July 2014 at 8:00 a.m. for two tests. The hydraulic and mechanical dredges work 8 h a day with a production capacity of dry mass $Q_s = 0.1388$ m³/h.

Numerous researchers have developed approaches for estimating resuspension rates associated with the typical operation of hydraulic and mechanical dredges, showing a very large range of possible values.

The mean resuspension factor R provided by the USEPA [35] is equal to 2.5% for the hydraulic dredge cutter head (T1); for test T2, a conservative mean resuspension factor R was taken to be 1% based on studies by [36] for releases from an environmental bucket dredge.

Moreover, following the literature data [37], the imposed mass flow rate of suspended solids was 5.56 kg/s for the hydraulic dredge (T1) and 3.44 kg/s for the mechanical dredge (T2). Table 1 summarises the model simulations.

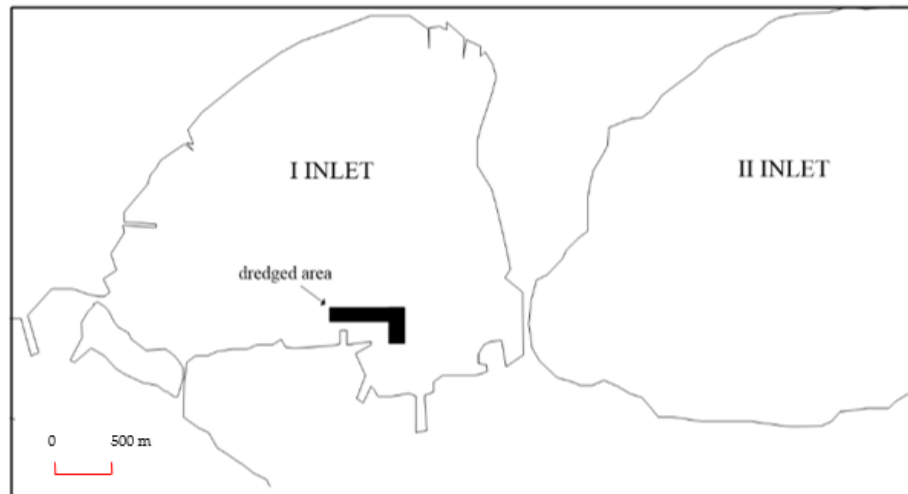


Figure 6. Dredged area.

Table 1. Parameters of the dredging implementation.

Parameters	T1	T2
Type of dredger	Hydraulic dredge	Ecological Mechanical dredge
Volume to be dredged (m ³)	50,000	50,000
Dredging time (d)	12	12
Production capacity (m ³ /h)	0.1388	0.1388
Mean resuspension factor R (%)	2.5	1.5

4. Results

Sea Circulation and Sediment Plume Dynamics

During a dredging activity, it is necessary to calculate the spatial distribution of SSC and to characterise sensitive resources (receptors). Therefore, a statistical analysis of the simulated parameters SSC is carried out to numerically estimate their spatial (vertical and horizontal) variability in order to have an evaluation of the potential environmental effects on the coastal area. For both type of dredges, the SSC_{max} distribution was studied for two different layers during the dredging activity.

Figures 7 and 8 represent the maps of SSC_{max} elaborated for the surface and bottom layers, respectively. The typical patterns, already observed by [38,39], are still evident, with a prevailing mean surface current outflowing from the basin during the dredging activity (Figure 7a). The dredged plume is transported from the dredged area towards the navigable channel, directed towards the Mar Grande (Figure 7b,c). Focusing on the bottom, the average current during the dredging activity inflows towards the Mar Piccolo Basin, as shown in Figure 8a. Generally, the reproduced velocity values are in the range 0.02–0.1 m/s, with some peaks (0.3 m/s) along the navigable channel of the Mar Piccolo.

The simulation output confirms the double-flux along the navigable channel and, further, proves the hydrodynamic mechanism of the water–mass exchange between the Mar Grande and the Mar Piccolo.

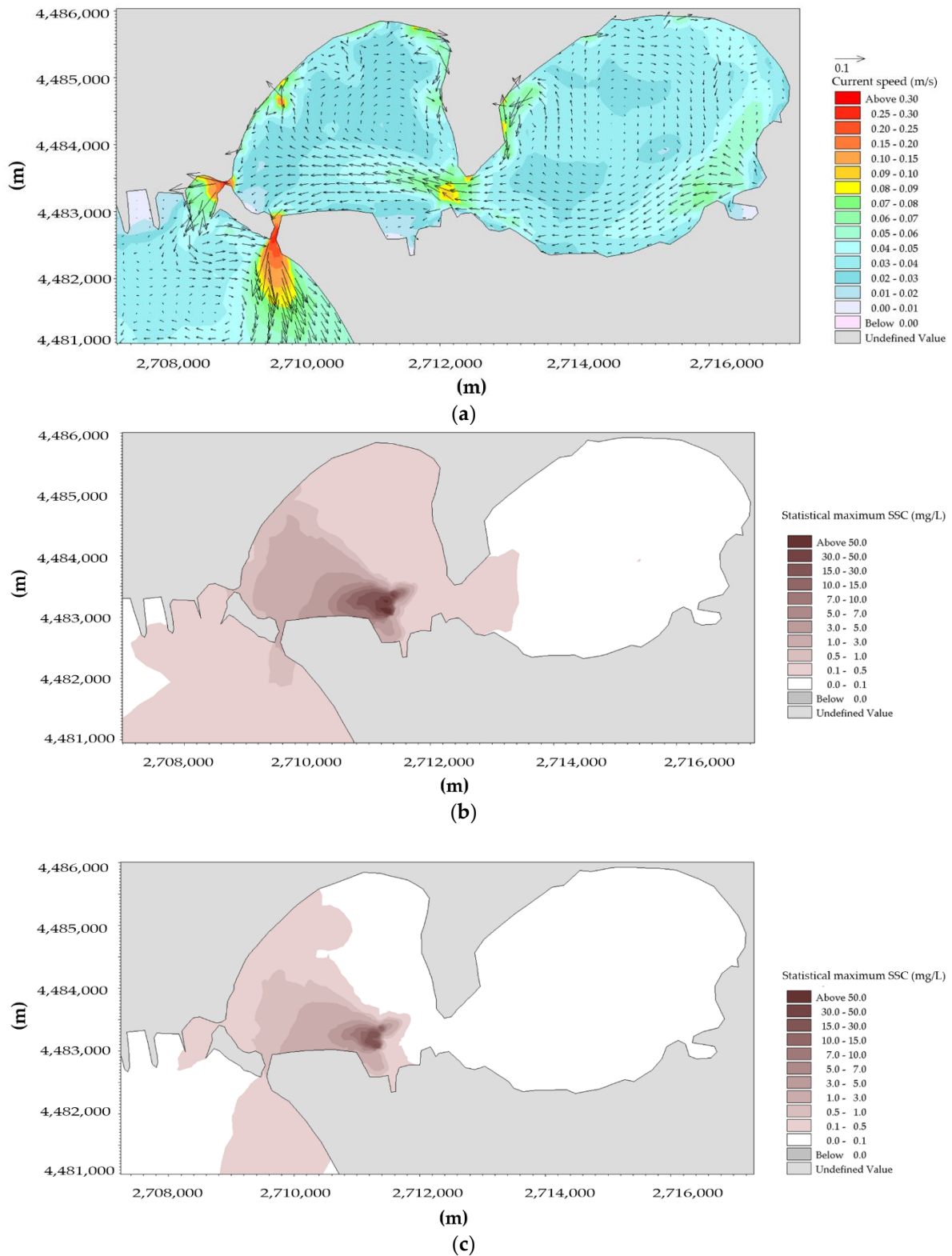


Figure 7. Computational maps of (a) the mean surface currents during the dredging activity, (b) SSC_{max} at the surface–hydraulic dredge and (c) SSC_{max} at the surface–mechanical dredge.

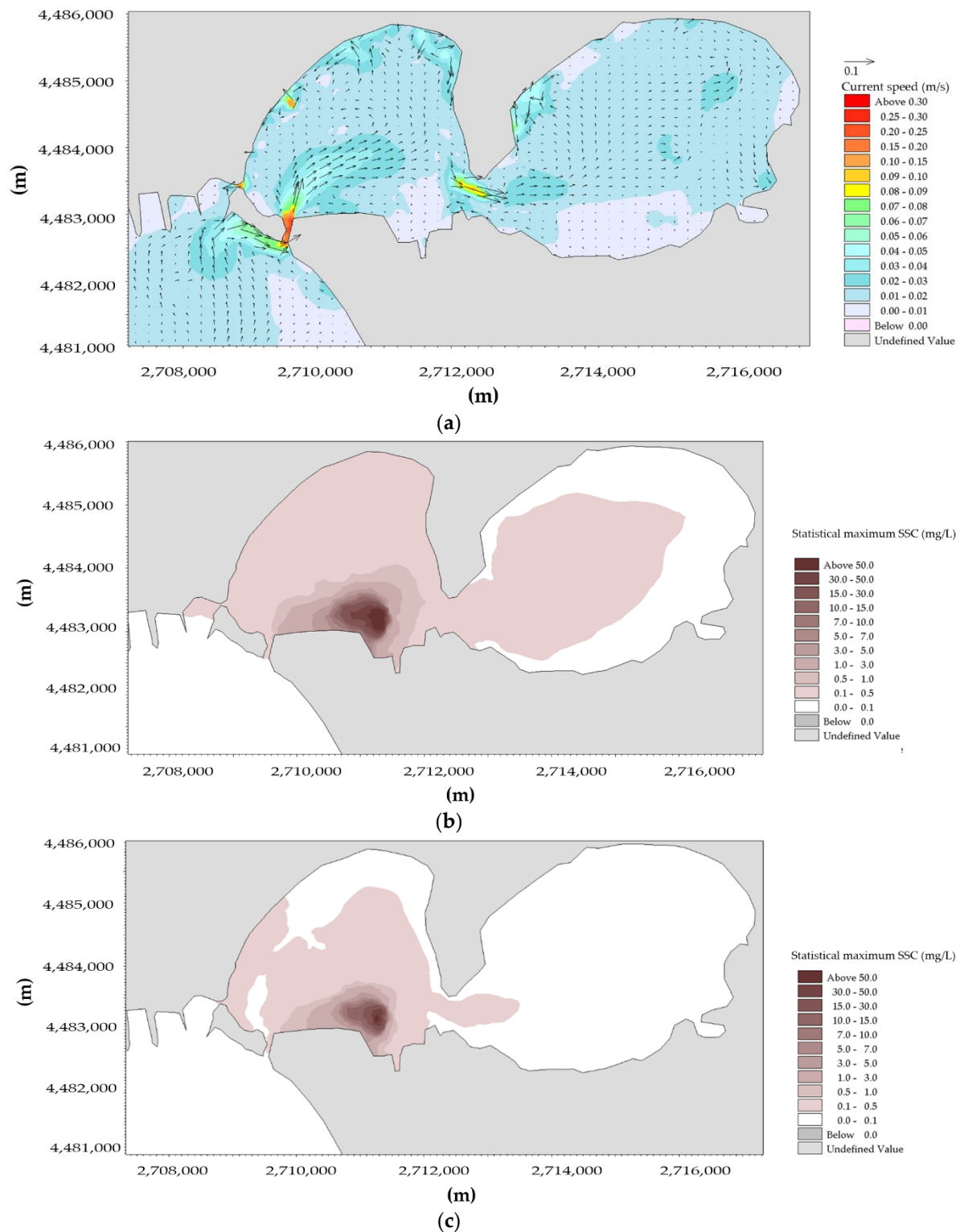


Figure 8. Computational maps of (a) the mean surface currents during the dredging activity, (b) SSC_{max} at the bottom–hydraulic dredge and (c) SSC_{max} at the surface–mechanical dredge.

Consequently, the Mar Piccolo Basin is seriously exposed to the plume pollution load. In fact, the plume is confined in Mar Piccolo Basin and reaches also Inlet II (Figure 8b,c).

Moreover, in the case of the hydraulic dredge, a higher intensity of the SSC_{max} in the immediate vicinity of the dredging point is shown at the surface and bottom layers (Figures 7a and 8a).

5. Discussion

Detecting Sensitive Areas around the Dredging Site

During the monitoring of a dredging activity, quantitative impact thresholds for the suspended solid concentration (SSC) must be established. In this study, a threshold of SSC was arbitrarily considered equal to 5 mg/L [40], and a regular grid of checkpoints (Figure 9) in the zone with a high impact was considered [41].

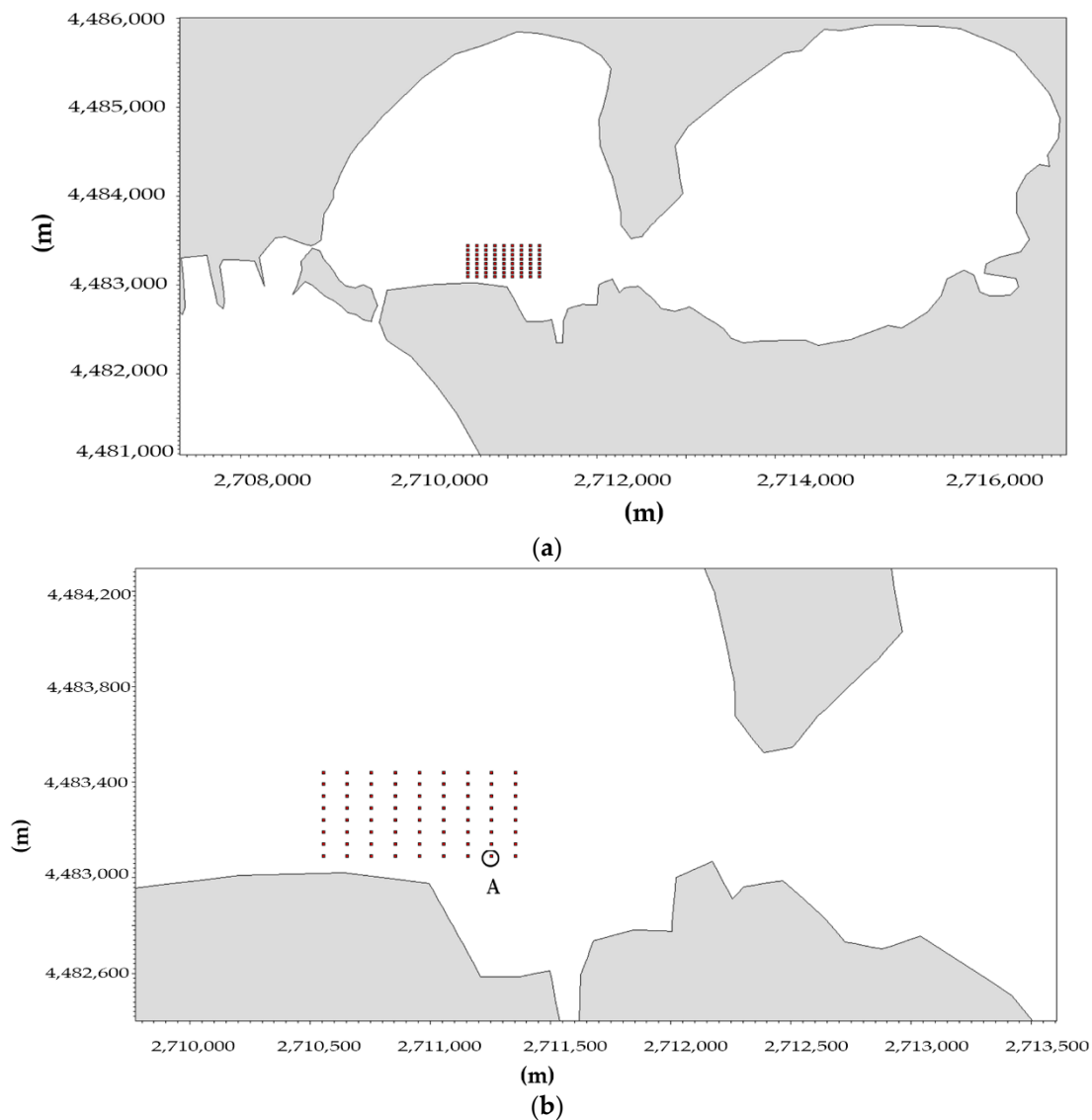


Figure 9. Location of discrete check points for result extractions: (a) whole area and (b) zoom.

For all checkpoints, starting from the SSC time series, the mean and maximum values (SSC_{mean} and SSC_{max}) were calculated (Figure 9).

According to Equation (1) by Feola et al. [40], the SSC_{num} —SSC number (mg s/L) was evaluated as the sum of the products of intensity and duration of the single events.

For the sake of brevity, only the checkpoint A, highlighted with a black circle in Figure 9b, is shown (Figures 10 and 11). Figure 12a,b shows the distribution of SSC_{num} for hydraulic and mechanical dredging plumes at the surface and bottom layers for all checkpoints (Figure 9).

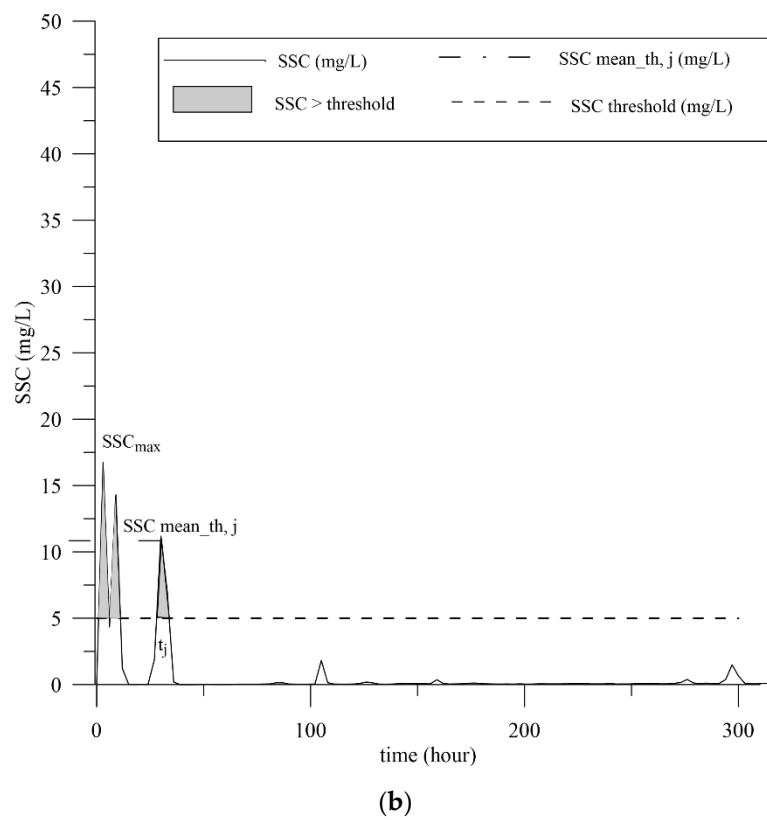
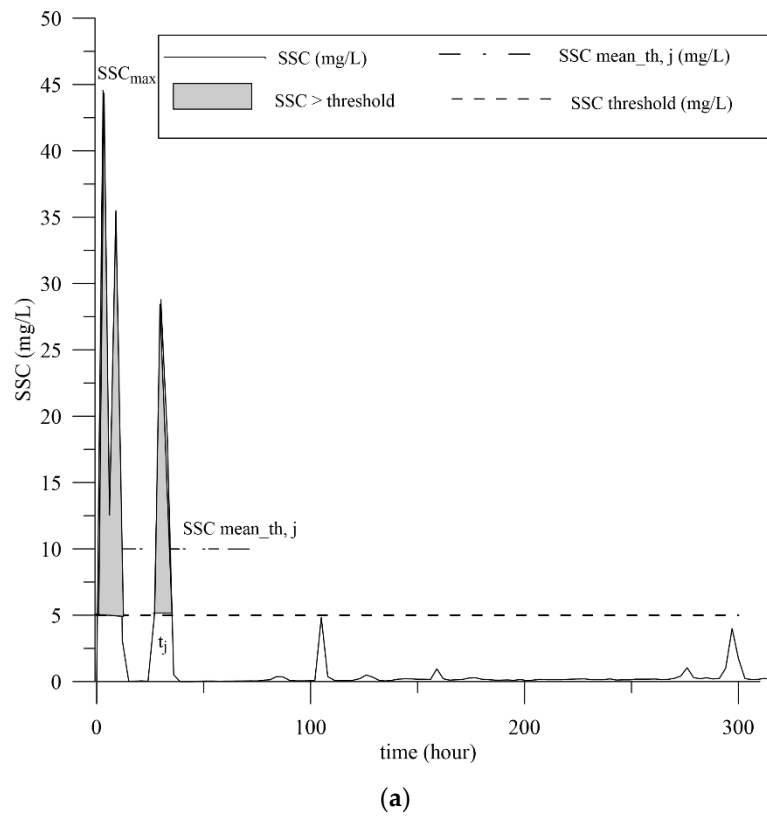
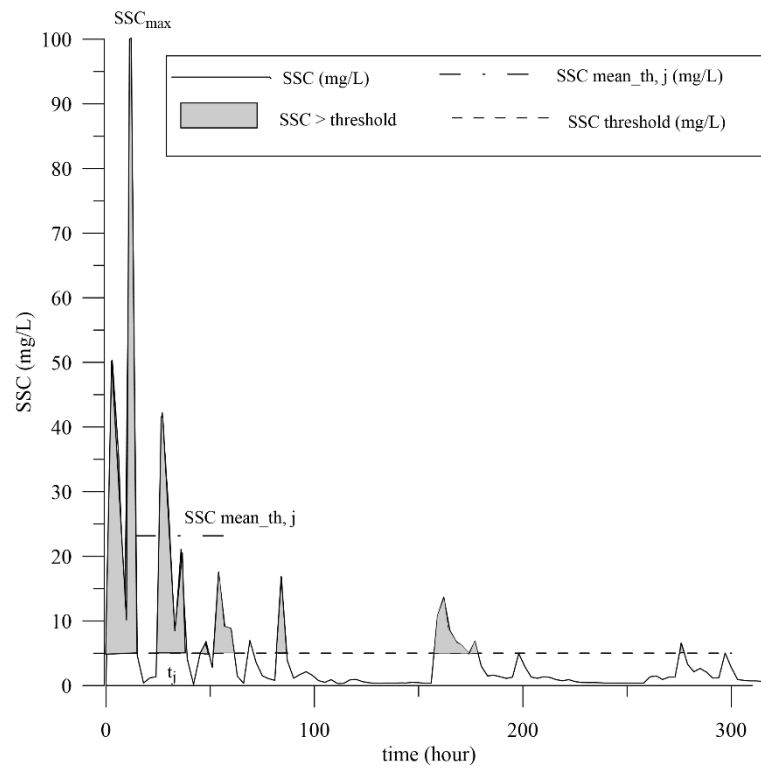
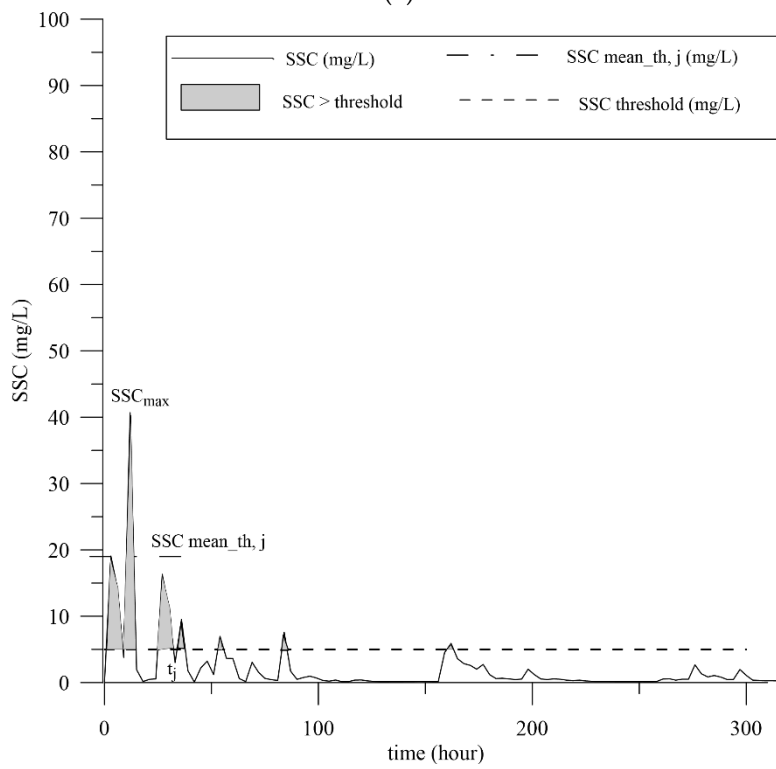


Figure 10. Point A: Time series for the SSC at the surface layer due to (a) hydraulic dredge and (b) mechanical dredge.



(a)



(b)

Figure 11. Point A: Time series for the SSC at the bottom layer due to (a) hydraulic dredge and (b) mechanical dredge.

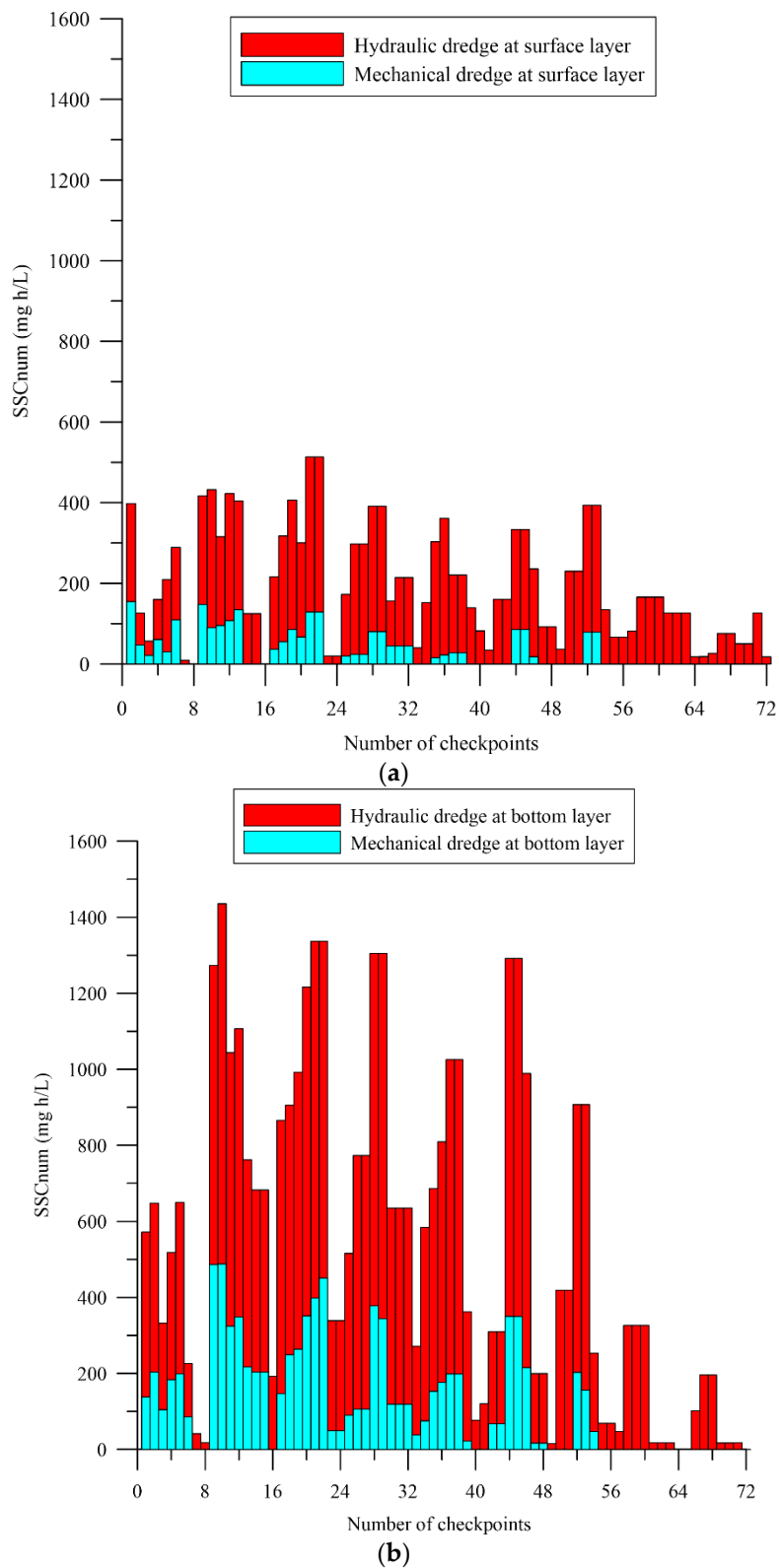


Figure 12. Distribution of the SSC number (SSC_{num}) for the mechanical and hydraulic dredging plumes at (a) the surface layer and (b) bottom layer.

Maps of the SSC_{num} distribution are shown for the hydraulic and mechanical dredgings at the surface and bottom layers (Figures 13 and 14).

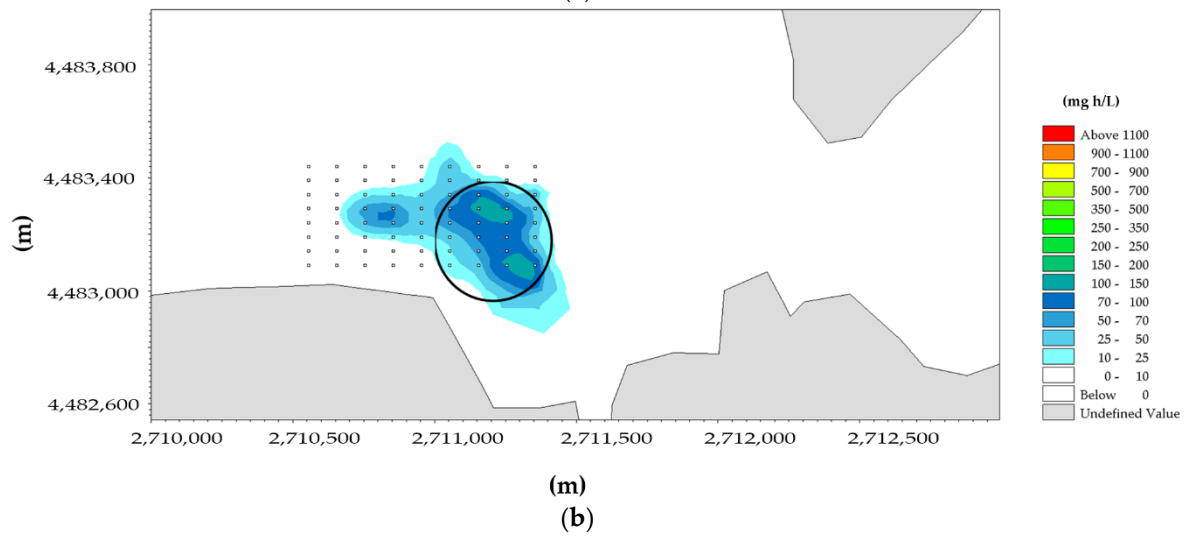
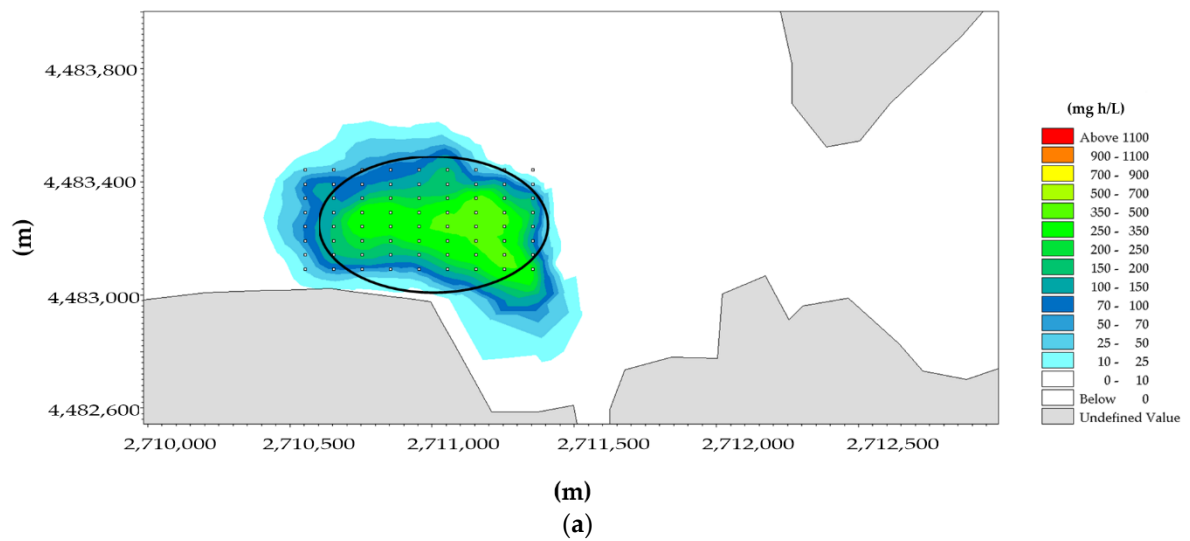


Figure 13. Distribution of the SSC_{num} at the surface layer due to (a) hydraulic dredge and (b) mechanical dredge.

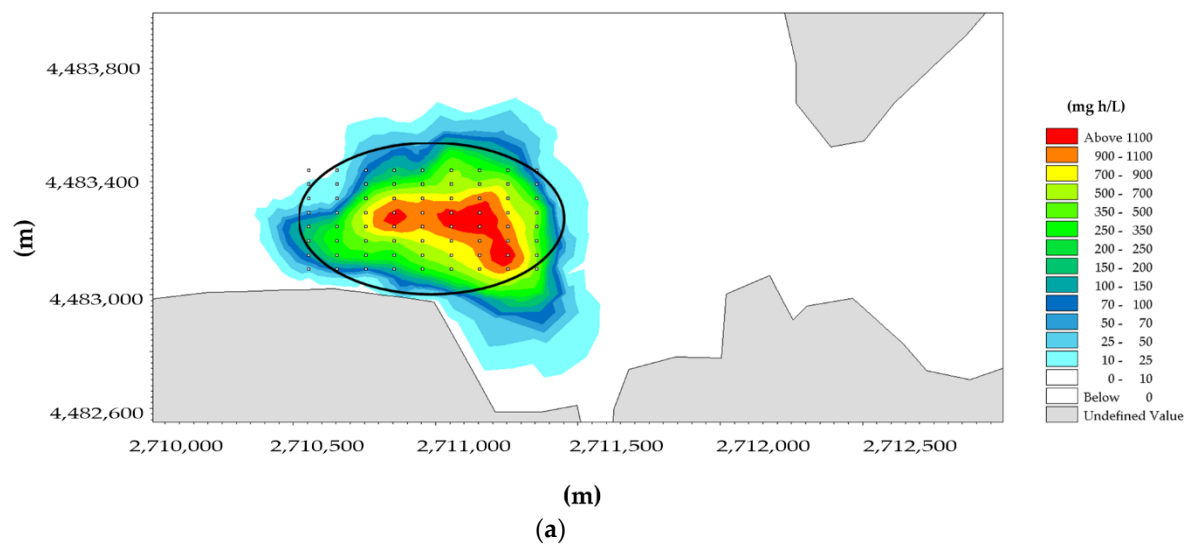


Figure 14. Cont.

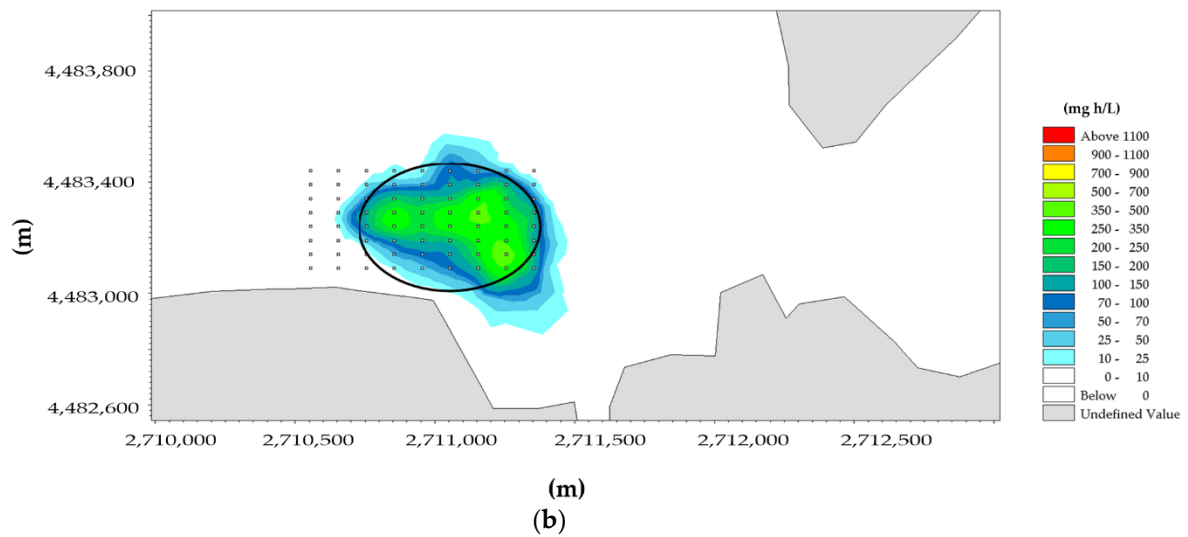


Figure 14. Distribution of the SSC_{num} at the bottom layer due to (a) hydraulic dredge and (b) mechanical dredge.

Figures 13a and 14a highlight a greater “affected” area in terms of the SSC_{num} variation at the surface and bottom layers, and therefore, the hydraulic dredging produces the worst conditions.

In order to study the effects of the plume dynamic as a function of distance from the dredging zone, the variogram function $\gamma(h)$ [42] was derived (Figure 9).

If the variogram reaches a limit value (sill), it means that there is a distance (range) beyond which the variable does not have spatial dependence (Figure 15).

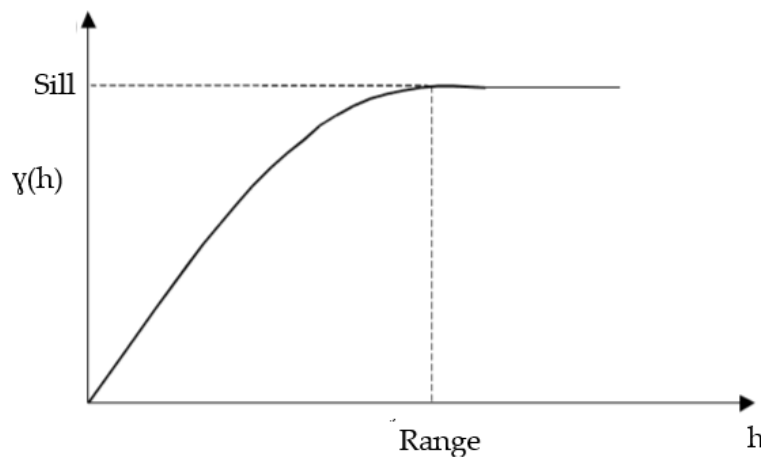


Figure 15. Variogram $\gamma(h)$ plot with indication of the sill and range parameters.

The variograms of the SSC_{num} presented in Figure 16 were obtained, for both hydraulic and mechanical dredges, at the surface and bottom layers.

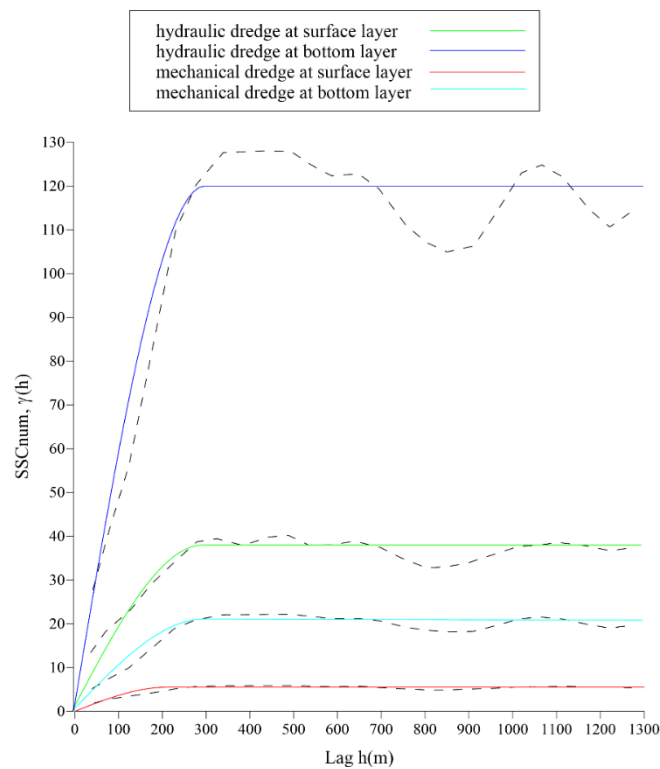


Figure 16. SSC_{num} variogram models evaluated at the surface layer due to (a) hydraulic dredge and (b) mechanical dredge.

By analysing Figure 16, the experimental variogram starts out straight, then bends over sharply and levels out; therefore, the spherical model matches in a better way the shape of the empirical variogram $\gamma(h)$.

Considering the relative differences for contiguous values lower than 5×10^{-1} , the spatial extent of the bottom layer SSC_{num} correlation can be identified around 1300 m and 700 m for hydraulic and mechanical dredges, respectively (Table 2).

Table 2. Sill and range values for the suspended solid concentration number (SSC_{num}) variogram models evaluated for mechanical and hydraulic dredges at the surface and bottom layers.

	Hydraulic Dredge		Mechanical Dredge	
	Surface	Bottom	Surface	Bottom
Sill	37	120	5.5	21
Range (m)	850	1300	380	700

Using the same criterion, the spatial extent of the surface layer SSC_{num} correlation can be identified around 850 m and 380 m for hydraulic and mechanical dredges, respectively (Table 2).

Coherently with the maps of the SSC_{num} distribution (Figure 13a,b), this result highlighted that the most dangerous conditions are observed for hydraulic dredge at the bottom layer.

Choosing a SSC_{num} meaningful threshold equal to $100 \text{ mg/L} \times h$, circles that can be considered as the limit between “not affected” and “affected” areas are introduced in Figures 13a and 14b.

The diameters of the circles are about 1300 m and about 700 m at the bottom layer and about 850 m and about 380 m at the surface layer for hydraulic and mechanical dredges, corresponding to the range shown by the variograms analysis.

6. Conclusions

The numerical model MIKE 3D FM MT was implemented to evaluate the response of the Mar Piccolo Basin to a hypothetical dredging activity during the spring season. To reproduce the sea circulation structure in the target area, a calibrated MIKE 3D FM model was used.

Environmental improvements to dredging techniques have become increasingly important over the last 25 years. Therefore, two simulation runs, denoted as T1 and T2, were carried out with the aim of comparing the effects due to two different dredges (i.e., hydraulic dredge cutter head and environmental mechanical bucket dredge).

A statistical analysis of the simulated parameter SSC was carried out to numerically estimate its spatial (vertical and horizontal) variability, thereby allowing an evaluation of the potential environmental effects on the coastal area.

For both types of dredges, the SSC_{max} variability distribution was evaluated at the surface and bottom.

In the case of a hydraulic dredge, a higher intensity of SSC_{max} in the immediate vicinity of the dredging point is shown at the surface and bottom layers. For both tests, T1 and T2, at the surface level, the dredged plume is transported from the dredged area towards the navigable channel of the Mar Piccolo, directed towards the Mar Grande Sea. Confined at the bottom the plume is the Mar Piccolo Basin, reaching also Inlet II.

Although, for careful management during a dredging activity, site-specific evaluations must be carried out, in this case study, a preliminary SSC threshold and an integrated index, SSC_{num} , were proposed.

Moreover, to study the effects of the plume dynamics due to two different dredges as a function of distance from the dredging zone, a geostatistical analysis of function SSC_{num} was carried out.

In this way, the variogram upper-bound value (sill) was used to estimate the severity of the effects. Table 2 shows that the most dangerous conditions are shown for hydraulic dredge at the bottom layer. It is evident that the correct prediction of contaminant transport depends on the reliability of the input data, as well as on the calibration made.

Author Contributions: M.M. devised and funded the research, M.M. conceived and coordinated the monitoring activities and D.D.P. performed the numerical modelling and analysed the results. D.D.P., M.B.M., F.D.S. and M.M. discussed and revised the paper. All authors have read and agreed to the published version of the manuscript.

Funding: This research received no external funding.

Acknowledgments: The monitoring stations were set up in the framework of the RITMARE Project and with funds from PON R&C 2007–2013.

Conflicts of Interest: The authors declare that there is no conflict of interest regarding the publication of this article.

References

1. Demars, K.R.; Richardson, G.N.; Raymond, N.Y.; Ronald, C. *Remediation, and Containment of Contaminated Sediments*; ASTM International: West Conshohocken, PA, USA, 1995.
2. John, S.A. *Scoping the Assessment of Sediment Plumes from Dredging*; CIRIA: London, UK, 2000.
3. Palermo, M.R.; Averett, D.E. Environmental dredging—A state of the art review. In Proceedings of the 2nd International Symposium on Contaminated Sediments: Characterization, Evaluation, Mitigation/Restoration, Management Strategy Performance, Quebec City, QC, Canada, 26–28 May 2003; pp. 12–17.
4. US Army Corps of Engineers (USACE). *A Review of Environmentally Improved Techniques for Dredging Contaminated Mud*; TECHNICAL NOTE TN 3/2003; Fill Management Division GEO: Hong Kong, China, 2003; p. 29.
5. Eisma, D. *Dredging in Coastal Water*; Taylor & Francis Publishing: London, UK, 2006; p. 244. ISBN 978-0-415-39111-5.
6. Bridges, T.S.; Gustavson, K.E.; Schroeder, P.; Ells, S.J.; Hayes, D.; Nadeau, S.C.; Palermo, M.R.; Patmont, C. Dredging processes and remedy effectiveness: Relationship to the 4 Rs of environmental dredging. *Integr. Environ. Assess. Manag.* **2010**, *6*, 619–630. [[CrossRef](#)] [[PubMed](#)]

7. Chimienti, G.; De Padova, D.; Mossa, M.; Mastrototaro, F. A mesophotic black coral forest in the Adriatic Sea. *Sci. Rep.* **2020**, *10*, 8504. [[CrossRef](#)] [[PubMed](#)]
8. De Carolis, G.; Adamo, M.; Pasquariello, G.; De Padova, D.; Mossa, M. Quantitative characterization of marine oil slick by satellite near-infrared imagery and oil drift modelling: The Fun Shai Hai case study. *Int. J. Remote Sens.* **2013**, *34*, 1838–1854. [[CrossRef](#)]
9. De Padova, D.; Mossa, M.; Adamo, M.; De Carolis, G.; Pasquariello, G. Synergistic use of an oil drift model and remote sensing observations for oil spill monitoring. *Environ. Sci. Pollut. Res.* **2017**, *24*, 5530–5543. [[CrossRef](#)]
10. Armenio, E.; Ben Meftah, M.; De Padova, D.; De Serio, F.; Mossa, M. Monitoring System in Mar Grande Basin (Ionian Sea). In Proceedings of the IEEE International Workshop on Metrology for the Sea, Learning to Measure Sea Health Parameters (Metrosea), Bari, Italy, 8–10 October 2019; pp. 104–109. [[CrossRef](#)]
11. Armenio, E.; Ben Meftah, M.; De Padova, D.; De Serio, F.; Mossa, M. Monitoring Systems and Numerical Models to Study Coastal Sites. *Sensors* **2019**, *19*, 1552. [[CrossRef](#)]
12. Great Barrier Reef Marine Park Authority (GBRMPA). *Guidelines: The Use of Hydrodynamic Numerical Modelling for Dredging Projects in the Great Barrier Reef Marine Park*; Great Barrier Reef Marine Park Authority (GBRMPA): Townsville, Australia, 2012; p. 8. Available online: <http://hdl.handle.net/11017/970> (accessed on 10 October 2020).
13. Lisco, S.; Corselli, C.; De Giosa, F.; Mastronuzzi, G.; Moretti, M.; Siniscalchi, A.; Marchese, F.; Bracchi, V.; Tessarolo, C.; Tursi, A. Geology of Mar Piccolo, Taranto (southern Italy): The physical basis for remediation of a polluted marine area. *J. Maps* **2016**, *12*, 173–180. [[CrossRef](#)]
14. Sollecito, F.; Cotecchia, F.; Mali, M.; Miccoli, D.; Vitone, C. Geo-chemo-mechanical characterization of a polluted marine basin. *E3S Web Conf.* **2019**, *92*, 18001. [[CrossRef](#)]
15. De Serio, F.; Armenio, E.; Ben Meftah, M.; Capasso, G.; Corbelli, V.; De Padova, D.; De Pascalis, F.; Di Bernardino, A.; Leuzzi, G.; Monti, P.; et al. Detecting sensitive areas in confined shallow basins. *Environ. Model. Softw.* **2020**, *126*, 104659. [[CrossRef](#)]
16. Labianca, C.; De Gisi, S.; Todaro, F.; Notarnicola, M. DPSIR model applied to the remediation of contaminated sites. A case study: Mar Piccolo of Taranto. *Appl. Sci.* **2020**, *10*, 5080. [[CrossRef](#)]
17. Cardelicchio, N.; Annicchiarico, C.; Di Leo, A.; Giandomenicom, S.; Spada, L. The Mar Piccolo of Taranto: An interesting marine ecosystem for the environmental problems studies. *Environ. Sci. Pollut. Res.* **2016**, *23*, 12495–12501. [[CrossRef](#)]
18. Vatova, A. Osservazioni fisico chimiche periodiche nel Mar Grande e Mar Piccolo di Taranto (1962–1969). *Boll. Pesca Piscic. Idrobiol.* **1972**, *XXVII*, 43–79.
19. Cerruti, A. *Le sorgenti sottomarine (Citri) del Mar Grande e nel Mar Piccolo di Taranto*; Annali Istituto Superiore Navale: Napoli, Italy, 1948; Volume 7, pp. 171–196.
20. Strusi, A.; Pastore, M. Osservazioni idrografiche del Mar Grande e nel Mar Piccolo di Taranto. Campagna 1970–71. *Oebalia* **1975**, *17*, 1–64.
21. De Serio, F.; Mossa, M. Environmental monitoring in the Mar Grande basin (Ionian Sea, Southern Italy). *J. Environ. Sci. Pollut. Res.* **2016**, *23*, 12662–12674. [[CrossRef](#)] [[PubMed](#)]
22. De Serio, F.; Mossa, M. Assessment of hydrodynamics, biochemical parameters and eddy diffusivity in a semi-enclosed Ionian basin. *Deep Sea Res. Part II Top. Stud. Oceanogr.* **2016**, *133*, 176–185. [[CrossRef](#)]
23. Armenio, E.; Ben Meftah, M.; Bruno, M.F.; De Padova, D.; De Pascalis, F.; De Serio, F.; Di Bernardino, A.; Mossa, M.; Leuzzi, G.; Monti, P. Semi enclosed basin monitoring and analysis of meteo, wave, tide and current data. In Proceedings of the IEEE Conference on Environmental, Energy and Structural Monitoring Systems, Bari, Italy, 13–14 June 2016. [[CrossRef](#)]
24. Armenio, E.; De Serio, F.; Mossa, M. Analysis of data characterizing tide and current fluxes in coastal basins. *Hydrol. Earth Syst. Sci.* **2017**, *21*, 3441–3454. [[CrossRef](#)]
25. Armenio, E.; De Serio, F.; Mossa, M.; De Padova, D. Monitoring system for the sea: Analysis of meteo, wave and current data. In Proceedings of the IMEKO TC19 Workshop on Metrology for the Sea, MetroSea: Learning to Measure Sea Health Parameters, Naples, Italy, 11–13 October 2017; pp. 143–148, ISBN 978-151085211-2.
26. De Padova, D.; De Serio, F.; Mossa, M.; Armenio, E. Investigation of the current circulation offshore Taranto by using field measurements and numerical model. In Proceedings of the 2017 IEEE International Instrumentation and Measurement Technology Conference, Turin, Italy, 22–25 May 2017; ISBN 978-1-5090-3596-0. [[CrossRef](#)]

27. De Serio, F.; Mossa, M. Meteo and Hydrodynamic Measurements to Detect Physical Processes in Confined Shallow Seas. *Sensors* **2018**, *18*, 280. [[CrossRef](#)]
28. DHI. *Mike 3 Flow Model: Hydrodynamic Module—Scientific Documentation*; DHI Software: Hørsholm, Denmark, 2016.
29. Simoncelli, S.; Fratianni, C.; Pinardi, N.; Grandi, A.; Drudi, M.; Oddo, P.; Dobricic, S. Mediterranean Sea Physical Reanalysis (CMEMS MED-Physics) [Data Set]. Copernicus Monitoring Environment Marine Service (CMEMS). 2019. Available online: https://doi.org/10.25423/MEDSEA_REANALYSIS_PHYS_006_004 (accessed on 10 October 2020).
30. Xie, P.; Arkin, P.A. Global precipitation: A 17-year monthly analysis based on gauge observations, satellite estimates, and numerical model outputs. *Bull. Am. Meteorol. Soc.* **1997**, *78*, 2539–2558. [[CrossRef](#)]
31. Rodi, W. Examples of calculation methods for flow and mixing in stratified fluids. *J. Geophys. Res. Ocean.* **1987**, *92*, 5305–5328. [[CrossRef](#)]
32. Smagorinsky, J. Large eddy simulation of complex engineering and geophysical flows. In *Evolution of Physical Oceanography*; Galperin, B., Orszag, S.A., Eds.; Cambridge University Press: New York, NY, USA, 1993; pp. 3–36.
33. Partheniades, E. Erosion and deposition of cohesive soils. *J. Hydraul. Div.* **1965**, *91*, 105–139.
34. Lumborg, U. Modelling the deposition, erosion, and flux of cohesive sediment through Øresund. *J. Mar. Syst.* **2005**, *56*, 179–193. [[CrossRef](#)]
35. USEPA. *Contaminated Sediment Remediation Guidance for Hazardous Waste Sites*; OSWER 9355.0-85; Office of Solid Waste and Emergency Response, U.S. Environmental Protection Agency: Washington, DC, USA, 2005. Available online: <http://www.epa.gov/superfund/resources/sediment/guidance.htm> (accessed on 10 October 2020).
36. Finch, M.; Fisher, R.; Palmer, A.; Baumgard, A. An Integrated Approach to Pipeline Burial in the 21st Century. In Proceedings of the Deep Offshore Technology 2000 Conference, New Orleans, LA, USA, 7–9 November 2000.
37. Hayes, D.; Wu, P.Y. Simple approach to TSS source strength estimates. In Proceedings of the Western Dredging Association Twenty-first Technical Conference and Thirty-third Annual Texas A and M Dredging Seminar Special PIANC Session/Texas A and M University, Center for Dredging Studies, Houston, TX, USA, 25 June 2001.
38. De Serio, F.; Mossa, M. Streamwise velocity profiles in coastal currents. *Environ. Fluid Mech.* **2014**, *14*, 895–918. [[CrossRef](#)]
39. De Pascalis, F.; Ghezzi, M.; Umgiesser, G.; De Serio, F.; Mossa, M. Use of SHYFEM open source hydrodynamic model for time scales analysis in a semi-enclosed basin. In Proceedings of the Environmental, Energy, and Structural Monitoring Systems (EESMS), Bari, Italy, 13–14 June 2016; pp. 1–4.
40. Feola, A.; Lisi, I.; Salmeri, A.; Venti, F.; Pedroncini, A.; Gabellini, M.; Romano, E. Platform of integrated tools to support environmental studies and management of dredging activities. *J. Environ. Manag.* **2016**, *166*, 357–373. [[CrossRef](#)] [[PubMed](#)]
41. SKM, Sinclair Knight Merz Pty Ltd. *Improved Dredge Material Management for the Great Barrier Reef Region*; Great Barrier Reef Marine Park Authority: Townsville, Australia, 2013.
42. Matheron, G. Principles of geostatistics. *Econ. Geol.* **1963**, *58*, e1246–e1266. [[CrossRef](#)]

Publisher’s Note: MDPI stays neutral with regard to jurisdictional claims in published maps and institutional affiliations.



© 2020 by the authors. Licensee MDPI, Basel, Switzerland. This article is an open access article distributed under the terms and conditions of the Creative Commons Attribution (CC BY) license (<http://creativecommons.org/licenses/by/4.0/>).